Journal of Magnetism and Magnetic Materials 374 (2015) 600–606

Contents lists available at ScienceDirect

Journal of Magnetism and Magnetic Materials

journal homepage: www.elsevier.com/locate/jmmm

Numerical studies of micromagnetic configurations in stripes with in-plane anisotropy and low quality factor

B.N. Filippov [a,b], M.N. Dubovik [a,b,*], V.V. Zverev [b]

[a] Institute of Metal Physics UB RAS, S. Kovalevskoy Str., 18, 620990 Yekaterinburg, Russia
[b] Ural Federal University, Mira Str., 19, 620002 Yekaterinburg, Russia

ARTICLE INFO

Article history:
Received 28 June 2014
Received in revised form
18 August 2014
Available online 10 September 2014

Keywords:
Micromagnetic simulation
Cross-tie domain walls
C-shaped domain walls
Permalloy films

ABSTRACT

Magnetization distributions and energy of 180-degrees domain walls in a stripe-film were investigated over a wide film thickness range. Three-dimensional numerical simulations are performed. Two kinds of transitions between stable domain wall configurations were obtained: from Néel walls to cross-tie walls and from cross-tie walls to asymmetric Bloch (C-shaped) walls. The latter kind of transition was investigated for the first time. The transition from the two-dimensional cross-tie structure to the three-dimensional one during the rise of the film thickness was demonstrated.

1. Introduction

Researchers have been paying a great attention to magnetic films with in-plane anisotropy and low quality factor $Q = K/2\pi M_S^2$ (M_S is the film saturation magnetization and K is the anisotropy constant). Information storage devices were developed based on those films evaporated on cylindrical surfaces with a small radius [1]. Nowadays interest increases in those films investigation. That is accounted for by both development of new film-based memory types with the extra high capacity, for instance "racetrack memory" [2,3], and a hope to reveal new physical properties. The hope is related to the new methods of films production and experimental investigation, and the theoretical numerical methods great development.

The film thickness was found to influence on the micromagnetic structures and thus on the film magnetization reversal. It was established long ago [4] that decreasing the film thickness results in arising a new type of domain wall: the Néel one. The situation was initially described as follows. At the film thickness $b > b_N$ one-dimensional (the magnetization vector $\mathbf{M}$ direction depends on one coordinate) Bloch walls were assumed to exist with the magnetization directed normally to the film surface in the wall center. At $b < b_N$ one-dimensional Néel walls are stable with the magnetization always parallel to the film surface. Both the one-dimensional walls possess symmetric structure relative to the wall center surface, with that surface being a plane. A domain wall center surface is the level surface $m_z = 0$ if the z axis is directed along the easy axis, where $\mathbf{m} = \mathbf{M}/M_S$ is a normalized magnetization. Thus the walls mentioned will be referred to as symmetric Néel and symmetric Bloch walls. The value b_N has been named as a Bloch–Néel transition thickness.

However Huber, Smith and Goodenough [5] observed the completely new cross-tie domain wall using the powder method. Later the cross-tie walls were also observed using the electron microscopy methods [6]. A cross-tie wall has the complicated structure with alternating vortexes and antivortexes on the film surface. Its energy was calculated to be lower than a Néel wall one in [7] but it was the case for all b values and the two different walls energies ratio was always equal to 0.6 independent on the film material parameters. That made the results of [7] strange. Notwithstanding many observations appeared of both Néel and cross-tie walls existing in the same conditions (see, for example, [8] and the references there). Attempts to improve the results of [7] using the more accurate (for that time) computation methods failed to clarify the matter thought gave new details about Néel walls [9–11]. There were also numerical simulations of a cross-tie wall structure [12,13] at a fixed b value.

Theoretical investigations [14–16] were more successful to reveal two points on the film thickness axis (instead of one b_N as in the previous theoretical concepts) where transitions occur between the different domain wall types. That agreed with the experimental results [17]. Let's refer the points mentioned as b_L and b_R (left and right, given the thickness increases while moving along the axis from left to right). b_L corresponds to the transition from Néel walls to cross-tie ones, and was obtained to be much

* Corresponding author at: Institute of Metal Physics UB RAS, S. Kovalevskoy Str., 18, 620990 Yekaterinburg, Russia.
E-mail addresses: filbor@imp.uran.ru (B.N. Filippov), dubovik@imp.uran.ru (M.N. Dubovik), vvzverev49@gmail.com (V.V. Zverev).

http://dx.doi.org/10.1016/j.jmmm.2014.09.011
0304-8853/

smaller than b_N. The thickness b_R was initially interpreted as the thickness above which symmetric Bloch walls became energetically favorable as compared with cross-tie ones. Thus cross-tie walls are stable at $b \in (b_L, b_R)$. However b_R determination in [14–16] has to be confessed incorrect now, because no one-dimensional symmetric Bloch walls exist in magnetically soft films according to the results of more recent numerical calculations [18–20]. Instead asymmetric Bloch walls (also referred to as C-shaped walls) and asymmetric Néel walls exist. The transition from the asymmetric domain walls to cross-tie walls was investigated in [19] but it was obtained that without applying a magnetic field the cross-tie wall energy was always smaller than the Néel wall one as it was in [7]. That again disagreed with the experimental data [8,17], and perhaps related to insufficiency of the Ritz method or of the trial functions used in [19].

There is one more point to be mentioned. On the one hand the one-dimensional model seems to be sufficient to study Néel walls in films much thinner than b_R. On the other hand according to [21] such walls can possess non-one-dimensional structure. Although the difference may be small at large computational cells number (see the next section), making no allowance for that may lead to unstable results. In this connection remember that according to [22] all one-dimensional magnetization distributions are unstable (see also [23], p. 163–164).

According to the mentioned above a clear picture of a one or another stable or metastable domain wall type existence at the different film thicknesses has not been obtained yet. We insist on that it is necessary to use the same calculation method for all the domain wall types to obtain such a picture. Nowadays three-dimensional calculation is available with making allowance for all necessary interactions including the long-range dipole–dipole one. The transition corresponding to b_L had already been investigated in such a way [24]. Here the results of the domain walls structure numerical investigations in the wider thickness range will be reported including the transition corresponding to b_R. This three-dimensional calculation results will be compared with the experimental observations of the cross-tie structure period dependence on the film thickness [25] (p. 424), and b_L and b_R values dependence on M_S and K [17]. At last it will be shown that the vortex and antivortex magnetization distributions cross-cutting the film in cross-tie walls became non-cross-cutting in asymmetric Bloch walls. This result has not been obtained yet theoretically or experimentally.

2. Simulation details

The simulations were performed using the OOMMF micromagnetic package [26]. A stripe-film fragment in the form of a parallelepiped is considered. The film surface is parallel to the xz plane and the easy axis is directed along the z axis (see Fig. 1). Thus let's denote the film width, thickness and length as a, b and c. The film magnetic state corresponds to two domains separated by a 180-degrees domain wall. To obtain the wall magnetization distribution the film energy minimization is performed with the condition for the magnetization vector $|\mathbf{M}| = M_S$. The total energy has the following form:

$$E = \int_0^a dx \int_0^b dy \int_0^c dz \left\{ \frac{A}{M_S^2} \nabla^2 \mathbf{M} + \frac{K}{M_S^2} \left(M_x^2 + M_y^2 \right) - \frac{1}{2} \mathbf{M} \mathbf{H}^{(m)} \right\} \qquad (1)$$

where the first, second and third terms in the integrand are the exchange, anisotropy and dipole–dipole interactions energy densities correspondingly. A is the exchange parameter and the stray field $\mathbf{H}^{(m)}$ is determined as follows:

$$\mathbf{H}^{(m)} = -\nabla \varphi, \quad \varphi(x,y,z) = \int_0^a dx' \int_0^b dy' \int_0^c dz' \mathbf{M}(x',y',z')$$

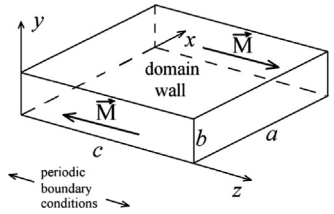

Fig. 1. Geometry of the problem. The considered stripe-film fragment and the domains magnetization directions are shown. The z axis is the easy magnetization axis and the y axis is directed normally to the film surface. The magnetization distribution $\mathbf{M}$ is treated as a function of the all three coordinates.

$$\nabla' \frac{1}{\sqrt{(x-x')^2 + (y-y')^2 + (z-z')^2}}. \qquad (2)$$

The features of implementing (2) in numerical calculations like performed here can be found in [27–29]. In brief, the computational region is divided by a grid into cubic cells, with each cell magnetization being considered uniform. After that the stray field is expressed as a convolution of the cells magnetization array with an interaction matrix determined by the grid and fast Fourier transforms are used to accelerate the calculation. If not stated otherwise, the following material parameters values are used: $A = 1.3 \times 10^{-6}$ erg/cm, $M_S = 800$ G, $K = 10^3$ erg/cm^3. The computational cells are cubic in shape, with an edge dimension equal to 5 nm.

The approach to cross-tie walls investigation is analogous to the one used in [24]. Cross-tie walls tend to possess periodic structure according to the existent experimental data and theoretic conceptions. Bearing that in mind one can use periodic boundary conditions applied along the easy axis direction (the z axis) to decrease the cells number and exclude the film edges effect. The periodic boundary conditions presence alters the exchange and magnetostatic energy calculation, namely, the magnetostatic interaction matrix is calculated in the different way [29]. Minimizing the energy of the initial $\mathbf{M}$ distribution roughly resembling a cross-tie wall structure one can obtain a stable equilibrium configuration for the fixed period c value. The initial distributions were created in such a way that the simulation region contains one vortex–antivortex pair (see Fig. 2). It is convenient to consider a domain wall energy surface density $\gamma_m = E_m / b \times c$. Here E_m is the equilibrium value of E and the energy is divided by b because as a rule all the interactions energies grow with increasing the film thickness and it is impossible to judge from E_m values how an interaction relative impact changes with the thickness change. With increasing the period c a cross-tie wall dependence $\gamma_m(c)$ converges asymptotically to the value corresponding to the Néel wall with the $\mathbf{M}$ distribution homogeneous along z. At small c values the wall energy density grows sharply due to the exchange energy increasing. In the intermediate c region the $\gamma_m(c)$ curve can have a minimum and that really takes place for the film thickness b larger than a certain value. This thickness value is b_L. The c value corresponding to the minimum mentioned is the "natural" cross-tie wall structure period T. The cross-tie wall would have this period in a film without any pinning centers and far from the film edges along the easy axis. The reader is referred to [24] for more details about T determination. One must obtain a new T value each time solving the problem with new parameters (the film thickness, material parameters, etc). If not stated otherwise, the data reported below corresponds to $c = T$. At $b < b_L$ the $\gamma_m(c)$ curve does not possess a minimum at any c value. In this case it is concluded that a pure Néel wall is stable at that film thickness.

As already mentioned the other domain wall types can exist in thicker films, namely asymmetric Bloch and Néel walls.

Performing the simulations to compare those walls energy with the cross-tie wall one, we assumed the asymmetric Bloch and Néel walls structure to be homogeneous along z. It was found (see for example [30]) that inhomogeneities in asymmetric Bloch wall structure along the easy axis (Bloch lines or singular points) increase the wall energy.

3. Results and discussion

Figs. 2 and 3 illustrate the **M** distribution in the cross-tie wall at the film thickness $b=20$ nm. Only one period along the z axis is shown containing one vortex and one antivortex on the film surface. In fact the wall core consists of the alternating Néel segments with the opposite magnetization rotation directions. This periodic structure leads to decreasing the magnetostatic energy as compared to a pure Néel wall, as Néel walls cores are sources of magnetostatic poles. That is seen clearly in Fig. 2b where div**m** is depicted. However vortex and antivortex **M** distributions (Fig. 2c) are formed necessarily at the Néel segments junctions. Antivortexes increase the magnetostatic energy and long cross-ties are formed near them to offset the increase slightly. These cross-ties are in fact domain walls perpendicular to the main wall. The cross-ties possess 90-degrees **M** rotation near the junction with the main wall core, and vanish gradually while moving into the domains. These ideas were reported yet in [5], and [24] contains their detailed and clear analysis and verification based on three-dimensional numerical simulation. The cross-tie in Fig. 2 is also a Néel wall as **m** rotates in the film plane.

The cross-tie wall structure period T is set by the magnetostatic and exchange interactions balance as decreasing (increasing) T leads exchange (magnetostatic) energy to grow. At $b<b_L$ the exchange interaction plays more important role than the magnetostatic one and a pure Néel wall becomes energetically favorable (the reader is referred to [24] for the details). Transition between the two domain walls types mentioned occurs by the way of increasing T with decreasing b as seen in Fig. 4. Our T calculations at the thicknesses closed to b_L are in a very good agreement with [24] despite we included the anisotropy interaction in the simulation. The obtained dependence $T(b)$ also agrees qualitatively

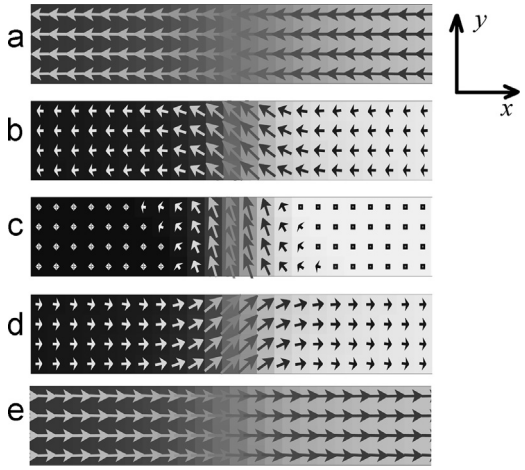

Fig. 3. Structure of the cross-tie domain wall in the z=const planes. The film dimensions are the same as in Fig. 2. The **m** distributions fragments at $z=200$ nm (a), $z=245$ nm (b), $z=250$ nm (c), $z=260$ nm (d), $z=300$ nm (e) are shown. The background color change from black to white corresponds to m_z change from -1 to $+1$.

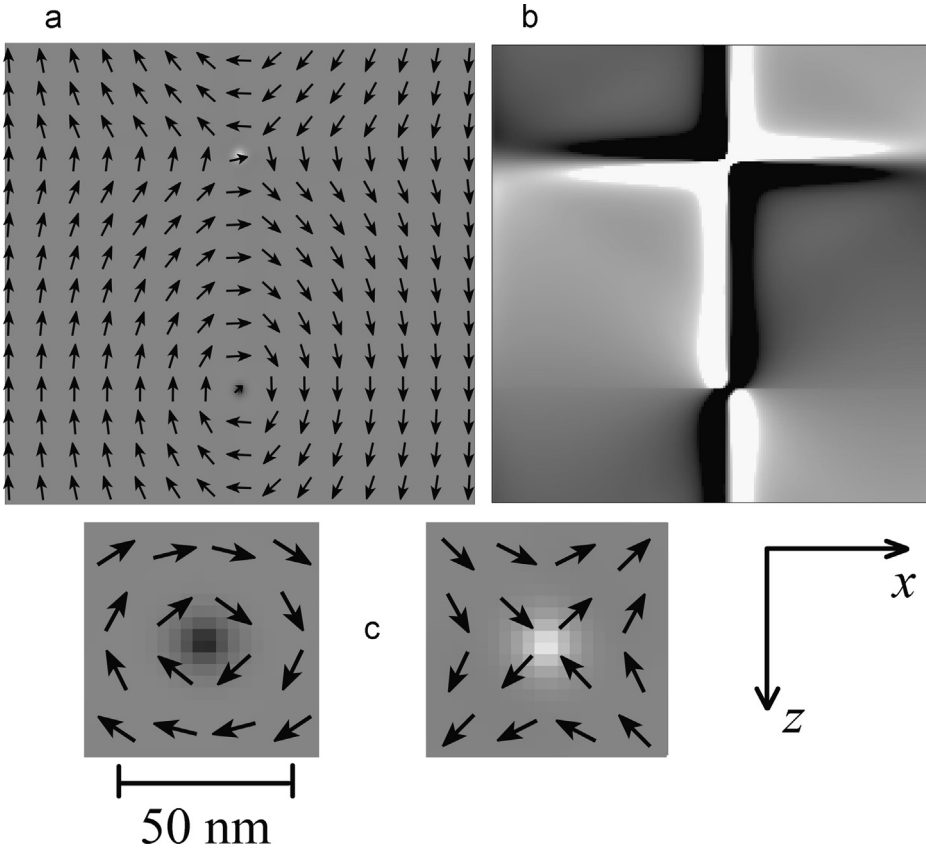

Fig. 2. Structure of the cross-tie domain wall on the film top surface. The film dimensions: $a=1000$ nm, $b=20$ nm, $c=1000$ nm (the "natural" cross-tie wall structure period T). The full magnetization distribution (a) and the zoomed vortex and antivortex (c) are shown, with the background color change from black to white corresponding to m_y change from -1 to $+1$. Given the background color corresponds to div**m** (the black/white one to the negative/positive value) the cross-tie is clearly seen (b).

with the experimental data [25]. Unfortunately a quantitative comparison cannot be performed as the films used in [25] had the widths more than 20 μm. In the present work the maximal stripe-film fragment width $a=2$ μm because of our current computational power. However the calculated dependence $T(a)$ (see Fig. 4) allows to make a suggestion about the T value approaching the experimental one with further increasing a.

Alternating vortexes and antivortexes on the film surface are probably the most unique cross-tie wall feature. Yet in the first cross-tie wall model [5] the vortexes and antivortexes cores were supposed to be magnetized normally to the film surface. Now that was confirmed experimentally [31,32]. Interesting that vortex core perpendicular magnetization was found firstly in permalloy dots [33] and then in films though for the latter ones the theoretical predictions had been made long before (see, for example, [14]). The significant delay in the experimental confirmation is accounted for by the small vortex core sizes (Fig. 2c). If the small core was not magnetized normally to the ferromagnetic vortex (antivortex) plane, prohibitive increasing the exchange energy would take place.

There is one more effect of varying the film thickness on a cross-tie wall structure besides change of T. The structure in Fig. 2 is almost uniform along the y axis. Only near the vortex and antivortex **M** shows slight dependence on y as was noted in [24]. According to our simulations the **M** distribution inhomogeneity through the film thickness enhances with increasing b as seen in Figs. 5 and 6. This structure has been obtained for the first time using three-dimensional simulation. The wall center line $m_z=0$ is strongly bent on the film surfaces as seen analyzing Fig. 6. Alternating Néel segments of the cross-tie wall now possess asymmetric structure similar to the asymmetric Néel walls obtained using two-dimensional simulations (see, for example, [19,20]). The difference is that according to the simulation results uniform along z asymmetric Néel walls possess two vortexes in the xy plane at the same film thickness and the other parameters (this **M** distribution is also called S-shaped wall). Described complication of the cross-tie wall structure is accounted for by the magnetostatic interaction role enhancement with increasing b along with that more inhomogeneous **M** distributions can be formed in thicker films without prohibitive increasing the exchange energy.

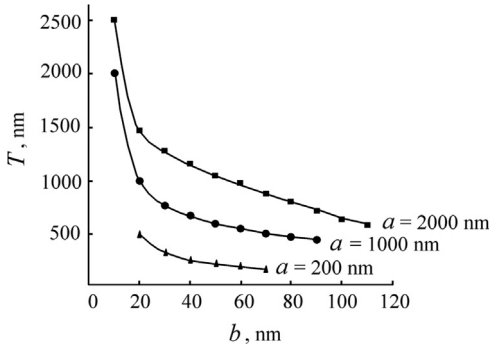

Fig. 4. Dependence of a cross-tie wall period T on the film thickness b for the different film width values. The points correspond to numerical results and the curves are a guide to an eye.

Fig. 7 illustrates the calculated dependences $\gamma_m(b)$ for the all domain walls types obtained at the given film parameters, namely: symmetric and asymmetric Néel walls, asymmetric Bloch walls (C-shaped), cross-tie walls. Any other domain wall types were not obtained. In Fig. 7 $b \in [5, 120]$ nm, nevertheless the film thicknesses up to 500 nm were considered. All the points on the cross-tie walls $\gamma_m(b)$ curve are obtained at $c=T(b)$. This film length value was also used while simulating the walls of the other types to verify their stability to transition into the cross-tie wall. The three-dimensional simulations give two transitions between stable domain wall configurations: b_L (from symmetric Néel walls to cross-tie ones) and b_R (from cross-tie walls to asymmetric Bloch ones). Of course, transitions between the metastable states can occur. For instance, C-shaped walls can exist also at the certain thickness range below b_R (see Fig. 7), up to about 40 nm. As well at $b > b_L$ symmetric Néel walls exist as metastable ones, gradually turning into asymmetric Néel walls. That is clearly seen from the corresponding curve $\gamma_m(b)$ starting to decrease with increasing b. To understand the reasons for that decrease let's take a look at Fig. 8 where the exchange and magnetostatic components of γ_m are shown as functions of b (the anisotropy component is not

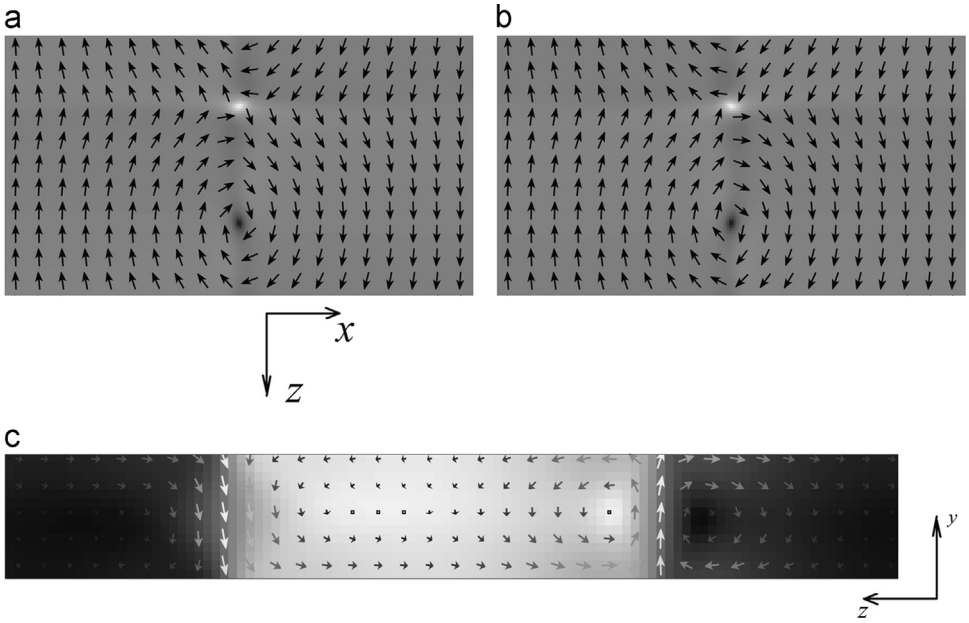

Fig. 5. Structure of the cross-tie domain wall. The film dimensions: $a=1000$ nm, $b=70$ nm, $c=500$ nm (the "natural" cross-tie wall structure period T). The full magnetization distributions on the film bottom (a) and top (b) surfaces and at the section $x=500$ nm (c) are shown. The background color change from black to white corresponds to m_y change from -1 to $+1$ (a) and (b) and to m_x change from -1 to $+1$ (c).

shown because it is always two orders of magnitude lower than the others). Asymmetric wall structure changes gradually with increasing b leading to a better magnetic flux closing and thus decreasing the magnetostatic component of γ_m. That decreases γ_m despite the exchange component of γ_m increases as a Néel wall becomes asymmetric and especially as the vortex magnetization distributions form in the xy-plane (compare Figs. 7 and 8). The similar behavior of the cross-tie walls $\gamma_m(b)$ curve is also accounted for by turning the symmetric Néel fragments of the wall into the asymmetric ones.

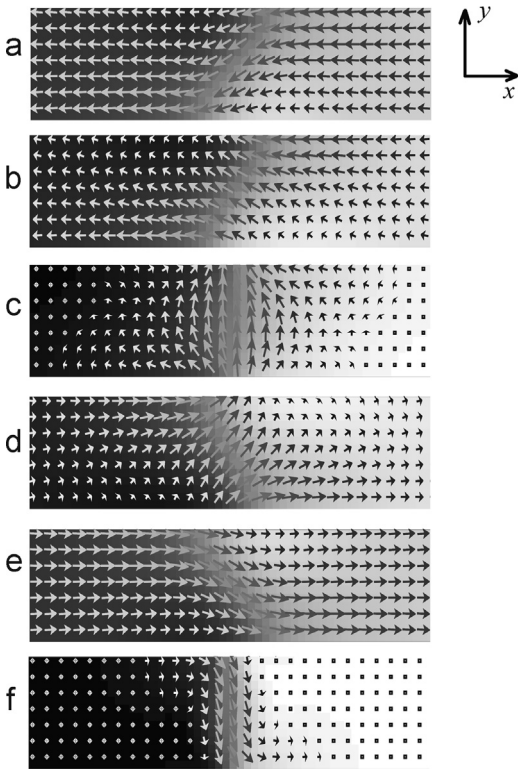

Fig. 6. Structure of the cross-tie domain wall in the z=const planes. The film dimensions are the same as in Fig. 5. The **m** distributions fragments at z=50 nm (a), z=110 nm (b), z=125 nm (c), z=140 nm (d), z=180 nm (e) z=375 nm (f) are shown. The background color change from black to white corresponds to m_z change from −1 to +1.

Finally the exchange energy densities corresponding to asymmetric Bloch and Néel walls start to decrease with increasing b. On the contrary cross-tie walls exchange energy density increases because of decreasing T and finally at $b > 90$ nm cross-tie walls become unstable. Asymmetric Bloch and Néel walls exist up to the largest thickness considered. The metastable configurations have a good stability and can exist really depending on the film magnetic history. We conclude that the metastable configurations existence is the reason for the different domain walls types observations at the seemingly identical conditions (see, for example, [8]). The value of b_L obtained (approximately 10 nm) is in a good agreement with [24]. The experimental b_L values are some higher (about 20 nm [17,25]). Reasons for that are still to be investigated. We suppose they may correspond to the large cross-tie structure period values for small film thicknesses.

The film width a value also exercises great influence on the different domain walls stability. In [24] decreasing the film width was found to increase b_L. According to our simulation decreasing a also leads to decreasing b_R as seen in Fig. 9a. Thus the smaller the film width a the narrower the thickness range of cross-tie walls stability (see Fig. 9b). The evident reason for that is cross-ties length limitation with the film narrowing along the x direction. With increasing the film width b_R approaches the value close to the experimental ones (about 90 nm [17,25]). One can see also in Fig. 9b that asymmetric Néel walls become unstable at the certain thickness of the film with a=200 nm. The structure with two vortexes in the xy-plane does not exist in this case despite it would decrease the magnetostatic energy due to a magnetic flux closing. In the narrow film where the wall cannot expand these energy savings would be less than the offset by increasing the exchange energy.

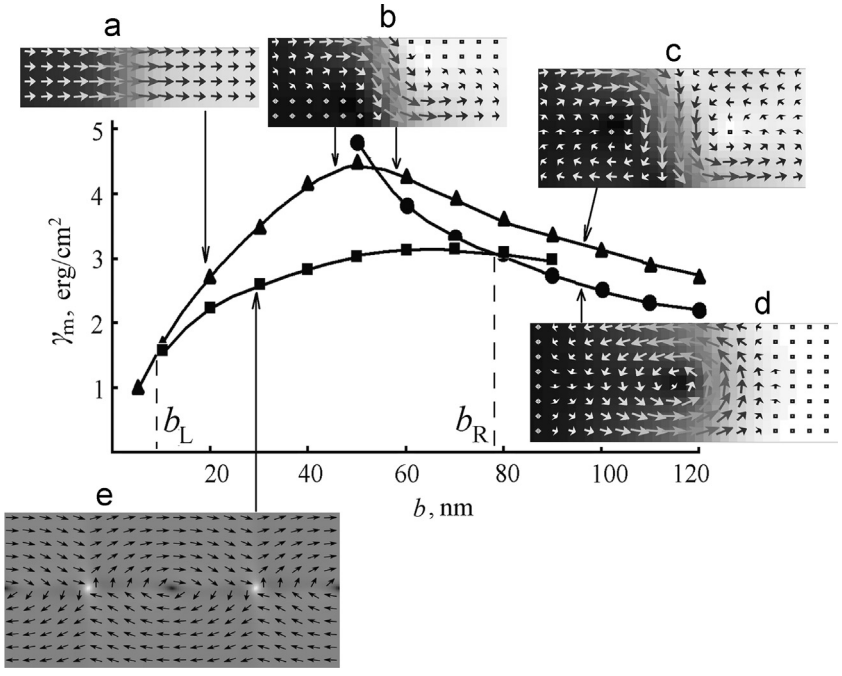

Fig. 7. Dependences of γ_m on the film thickness b for symmetric Néel walls (a), asymmetric Neel walls (b) and (c), asymmetric Bloch walls (d) and cross-tie walls (e). The film width a=1000 nm. The points correspond to numerical results and the curves are a guide to an eye.

The b_L and b_R values dependences on the material parameters M_S and K were calculated. The saturation magnetization was found to influence on the transition thicknesses values. It is seen in Fig. 10 that b_R (b_L) deviates slightly from the linear function of $1/M_S$ ($1/M_S^2$). That is in a qualitative agreement with that reported in [17]. It was found also that varying the anisotropy constant value K from 10^3 to 10^4 erg/cm^3 exercises negligible influence on b_L, b_R. On the other hand in [17] linear dependence of b_L on $\sqrt{K}/M_S^2$ was reported on. Obviously the reason for that discrepancy is that the authors of [17] could not consider the dependences $b_L(K)$ and $b_L(M_S)$ separately because of the films available, and clearly had an aim to fit their curves with Middelhoek's theory [7]. Also the difficulties in experimental measurement of b_L, b_R should be taken into account.

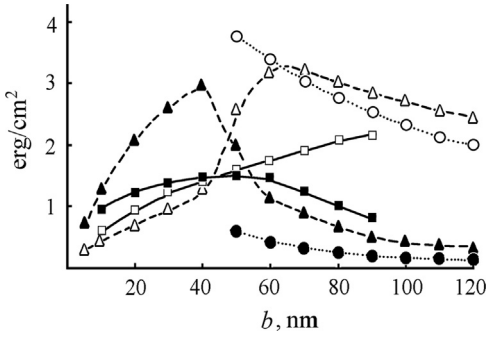

Fig. 8. Dependences of the magnetostatic (solid symbols) and exchange (open symbols) components of γ_m on the film thickness b for symmetric and asymmetric Néel walls (triangles), asymmetric Bloch walls (circles) and cross-tie walls (squares). The film width $a=1000$ nm. The points correspond to numerical results and the curves are a guide to an eye.

Finally let's turn our attention again to Figs. 2 and 5. The cross-tie walls vortexes and antivortexes on the film surface are cross-cutting the film. In other words, magnetization distribution has the vortex (antivortex) structure in the all film sections normal to the y-direction. Asymmetric Bloch-walls stable at $b > b_R$ can also possess vortex and antivortex **M** distributions on the film surfaces. That takes place at the junction of two asymmetric Bloch wall segments leading to a so-called Néel cap switch on the film surfaces (see, for example, [33]). A Néel cap switch is an attribute of Bloch-lines emerging when the two C-shaped wall segments possess the different xy-plane-vortex magnetization rotation directions and the vortexes on the same side of the $m_z=0$ level surface; or the different xy-plane-vortex magnetization rotation directions and the vortexes on the opposite sides of the $m_z=0$ level surface. The latter case is shown in Fig. 11.

In this case vortex or antivortex **M** distributions are also formed inevitably on the film surface, but they are non-cross-cutting. On the contrary in Fig. 11 the vortex on the top film surface corresponds to the antivortex on the bottom surface. The evident reason for that is the opposite **M** rotation directions in the top and bottom Néel fragments of an asymmetric Bloch wall. Thus one can come to conclusion that with increasing b the film surface vortexes and antivortexes changes their structure from the cross-cutting one to the non-cross-cutting one. Note that the described Bloch-

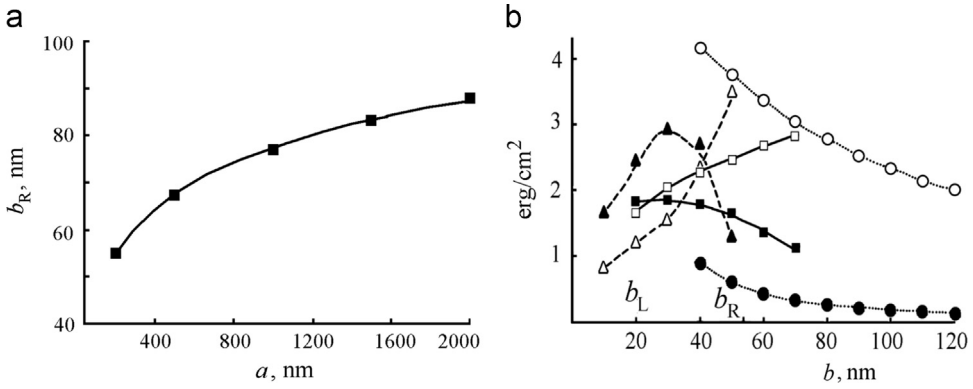

Fig. 9. Dependence of b_R on the film width (a). Dependences of the magnetostatic (solid symbols) and exchange (open symbols) components of γ_m on the film thickness b for the same domain walls types as in Fig. 8 (the same symbols refer to the same types of walls) at the film width $a=200$ nm (b). The points correspond to numerical results and the curves are a guide to an eye.

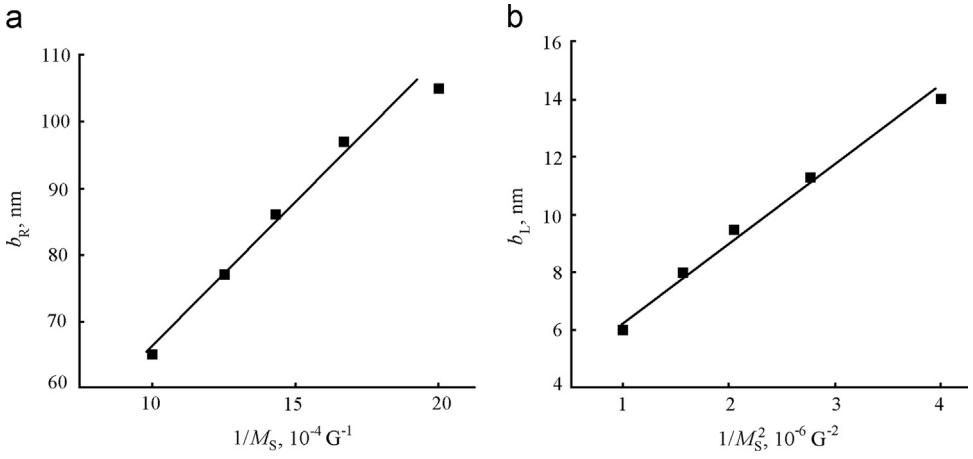

Fig. 10. Dependences $b_R(1/M_S)$ and $b_L(1/M_S^2)$. The points correspond to numerical results. The straight lines are drawn to compare the numerical data with the linear dependences reported in [7,17].

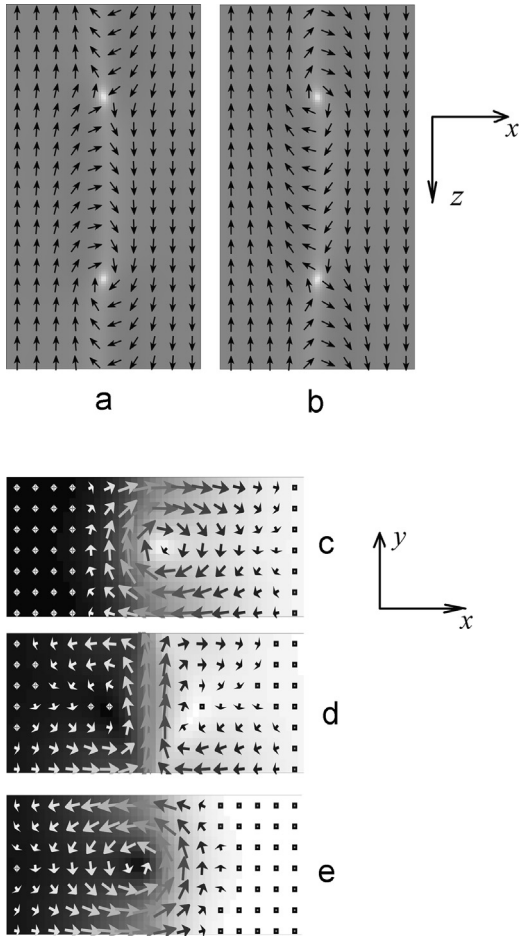

Fig. 11. Structure of the C-shaped domain wall with two vertical Bloch-lines. The film dimensions: $a=400$ nm, $b=100$ nm, $c=750$ nm. The full magnetization distributions on the film bottom (a) and top (b) surfaces and the **m** distributions fragments in the planes $z=0$ (c), $z=188$ nm (d), $z=375$ nm (e) are shown. The background color change from black to white corresponds to m_y change from -1 to $+1$ (a) and (b) and to m_z change from -1 to $+1$ (c)–(e).

lines on asymmetric Bloch walls are always metastable [31] but their existence is verified experimentally [25]. Fig. 11 contains also several cross-sections giving more information about the structure with a non-cross-cutting surface vortex/antivortex.

4. Conclusion

The energies and stability of the main domain walls types existing in magnetically soft films with in-plane anisotropy were investigated as a function of the film thickness b. Three-dimensional micromagnetic simulation was used. The main results obtained are the following ones:

Up to the very small thicknesses the only stable domain walls types in the films considered are cross-tie walls and asymmetric Bloch walls. Néel walls (symmetric and asymmetric) are metastable except at $b<b_L$ (about 10 nm depending on the film parameters).

There are two thicknesses corresponding to transitions between the stable domain wall types: from symmetric Néel walls to cross-tie ones (b_L) and then to asymmetric Bloch ones (b_R). The latter transition was investigated for the first time using three-dimensional simulation.

At any film thickness Bloch lines existence leads to formation of vortexes and antivortexes on the film surfaces. With increasing b those vortexes/antivortexes structures turn from cross-cutting to non-cross-cutting.

A qualitative agreement of cross-tie walls structure period T dependence on the film width and thickness; b_L and b_R dependence on M_S with the experimental data was obtained.

Cross-tie walls structure becomes three-dimensional with increasing b.

References

[1] L.A. Grigoryan, Memory devices at cylindrical magnetic films, Energy, Moscow (1975) (in Russian).
[2] S.S.P. Parkin, M. Hayashi, L. Thomas, Science 320 (2008) 190–194.
[3] M. Hayashi, L. Thomas, R. Moriya, C. Rettner, S.S.P. Parkin, Science 320 (2008) 209–211.
[4] L. Néel, Comptes rendus acad, Scienc 241 (1955) 533–536.
[5] E.E. Huber, D.O. Smith, J.B. Goodenoudh, J. Appl. Phys. 29 (1958) 294–295.
[6] E. Fuchs, Zs. Angew. Phus. 14 (1962) 203–208 (in German).
[7] S. Middelhoek, J. Appl. Phys. 34 (1963) 1054–1059.
[8] V.I. Petrov, G.V. Spivak, O.P. Pavlyuchenko, Sov. Phys. Usp. 15 (1972) 66–94.
[9] E. Feldtkeller, E. Fuchs, Zs. Angew. Phys. 18 (1964) 1–4 (in German).
[10] H. Riedel, A. Seeger, Phys. Status Solidi B 46 (1971) 377–384.
[11] A. Hubert, Phys. Status Solidi 38 (1970) 699–713.
[12] S. Huo, J. Bishop, J. Tucker, W. Rainforth, H. Davies, IEEE Trans. Magn. 33 (1997) 4170–4172.
[13] S. Huo, G. Pan, G.P Heydon, W.M. Rainforth, D.J. Mapps, W.W. Clegg, H.A. Davies, M.R. Gibbs, J. Appl. Phys. 87 (2000) 1096–1102.
[14] R.C. Collete, Domain Walls, Demagnetizing Fields and Anisotropy in Thin Ferromagnetic Films, Thesis, California Institute of Technology, Pfsadena, 1964.
[15] N. Minnaja, J. Phys. Colloques 32 (1971) C1–406.
[16] K.L. Metlow, J. Low Temp. Phys. 139 (2005) 207–219.
[17] S.U. Jen, S.P. Shieh, S.S. Liou, J. Magn. Magn. Mater. 147 (1995) 49–54.
[18] A.E. La Bonte, J. Appl. Phys. 40 (1969) 2450–2458.
[19] A. Hubert, Phys. Status Solidi A 32 (1969) 519–534.
[20] B.N. Filippov, J. Low Temp. Phys. 28 (2002) 707–738.
[21] V.S. Semenov, Phys. Met. Metall. 111 (2011) 441–450.
[22] W.F. Brown, S. Shtrikman, Phys. Rev. 123 (1962) 825–828.
[23] A. Aharoni, Introduction to the Theory of Ferromagnetism, Oxford University Press, Oxford, 2007.
[24] M.J. Donahue, Adv. Condens. Matter Phys. 2012, (2012), 908692.
[25] A. Hubert, R. Schafer, Magnetic Domains. The Analysis of Magnetic Microstructures, Springer, Berlin, Heidelberg, New York, 2009 (Corrected).
[26] M.J. Donahue, D.G. Porter, OOMMF User's Guide,Version 1.0 NISTIR 6376, National Institute of Standards and Technology, Gaithersburg, MD, 1999.
[27] A.J. Newell, W. Williams, D.J. Dunlop, J. Geophys. Res. Solid Earth 98 (1993) 9551–9555.
[28] M.E. Schabes, A. Aharony, IEEE Trans. Magn. 23 (1987) 3882–3888.
[29] K.M. Lebecki, M.J. Donahue, M.W. Gutowski, J. Phys. D: Appl. Phys 41 (2008) 175005.
[30] V.V. Zverev, B.N. Filippov, J. Exp. Theory Phys. 117 (2013) 108–120.
[31] K. Shigeto, T. Okuno, K. Mibu, T. Shingo, J. Appl. Phys. 80 (2002) 4190–4192.
[32] T. Shinjo, T. Okuno, R. Hassdorf, K. Shigeto, T. Ono, Science 289 (2000) 930–932.
[33] M. Redjdal, A. Kakay, M.F. Ruane, F.B. Humphrey, J. Appl. Phys. 91 (2002) 8278–8280.